Inorg. Chem. **2003**, *42*, 8674–8681

2,6-Di(pyrimidin-4-yl)pyridine Ligands with Nitrogen-Containing Auxiliaries: The Formation of Functionalized Molecular Clefts upon Metal Coordination

J. Frantz Folmer-Andersen, Hassan Aït-Haddou, Vincent M. Lynch, and Eric V. Anslyn*

Department of Chemistry and Biochemistry, The University of Texas at Austin, Austin, Texas 78701

Received July 14, 2003

A series of ligands (**1**–**4**) based on a 2,6-di(pyrimidin-4-yl)pyridine scaffold have been synthesized, and their abilities to form complexes with Zn(II) and Cu(II) have been determined using UV/vis spectroscopy in buffered aqueous solution (0.01 M *N*-[2-hydroxyethyl]piperazine-*N*′-[3-ethanesulfonic acid] (HEPES) at pH = 6.8). The Zn(II) complex of **1** was determined to have a formation constant of 8.4×10^3 M^{-1} while the formation constant of the Cu(II) complex was found to be 1×10^6 M^{-1}. The presence of auxiliary amines in **2** increased the stability of the Zn(II) complex relative to that of **1** by a factor of over 40, suggesting possible coordination of the auxiliaries to the Zn(II) center. The guanidinium and 2-amino-4,5-dihydro-imidazolinium groups of **3** and **4** considerably diminished the stability of the Zn(II) and Cu(II) complexes relative to those of **1**. X-ray crystal structures of **1-Zn**, **3-Zn**, **4**, and **4-Zn** were obtained and are discussed. A significant increase in the stability of **3-Zn**, but not in the stability **1-Zn**, was observed upon the addition of 1 equiv of sodium phosphate, implicating a stabilizing interaction of the guanidinium groups of **3-Zn** and the phosphate anion.

Introduction

Transition metal complexes of multidentate ligands have been widely used in modern chemical applications including catalyst development,[1−7] supramolecular self-assembly,[8−10] and anion recognition.[11−15] Transition metal ions provide structural rigidity to complexes of multidentate ligands through various coordination geometries,[16,17] and can serve as centers for noncovalent interactions[14,18−20] and chemical transformations.[1−7,21] The coordination of multidentate ligands to metal ions has recently been shown to affect polymer structure in organic−inorganic hybrid materials,[22] and to direct the aggregation of functionalized gold nanoparticles.[23] The introduction of auxiliary functional groups to the ligands of such systems has been utilized as a means of establishing preorganized recognition sites,[24] modulating supramolecular architectures,[25,26] and enhancing the reactivity of metal

* Author to whom correspondence should be addressed. E-mail: anslyn@ccwf.cc.utexas.edu.

(1) Young, M. J.; Chin, J. *J. Am. Chem. Soc.* **1995**, *117*, 10577.
(2) Gadja, T.; Krämer, R.; Jancsó A. *Eur. J. Inorg. Chem.* **2000**, 1635.
(3) Breslow, R.; Berger, D.; Huang, D.-L. *J. Am. Chem. Soc.* **1990**, *112*, 3686.
(4) Capacchione, C.; Proto, A.; Ebling, H.; Mülhaupt, R.; Möller, K.; Spaniol, T. P.; Okuda, J. *J. Am. Chem. Soc.* **2003**, *125*, 4954.
(5) Kang, S. O.; Kim, M. *J. Am. Chem. Soc.* **2003**, *125*, 4684.
(6) Shelton, V. M.; Morrow, J. R. *Inorg. Chem.* **1991**, *30*, 4295.
(7) Xu, X.; Lajmi, A., R.; Canary, J. W. *Chem. Commun.* **1998**, 2701.
(8) Bassani, D. M.; Lehn, J.-M.; Fromm, K.; Fenske, D. *Angew. Chem., Int. Ed.* **2002**, *41*, 4041.
(9) Dong, Y.-B.; Smith, M. D.; zur Loye, H.-C. *Inorg. Chem.* **2000**, *39*, 4927.
(10) Alves, W. A.; de Almeida, S. A.; de Almeida Santos, R. H.; Costa Ferreira, A. M. *Inorg. Chem. Commun.* **2003**, *6*, 294.
(11) Beer, P. D.; Hayes, E. J. *Coord. Chem. Rev.* **2003**, *240*, 167.
(12) Sun, S.-S.; Lees, A. J.; Zavalij, P. J. *Inorg. Chem.* **2003**, *42*, 3445.
(13) Lee, D. H.; Im, J. H.; Son, S. U.; Chung, Y. K.; Hong, J.-I. *J. Am. Chem. Soc.* **2003**, *125*, 7752.
(14) Tobey, S. L.; Jones, B. D.; Anslyn, E. V. *J. Am. Chem. Soc.* **2003**, *125*, 4026.
(15) Hasenknopf, B.; Lehn, J.-M.; Kneisel, B. O.; Baum, G.; Fenske, D. *Angew. Chem., Int. Ed. Engl.* **1996**, *35*, 1838.
(16) Linton, B.; Hamilton, A., D. *Chem. Rev.* **1997**, *97*, 1669.
(17) Lehn, J.-M. *Supramolecular Chemistry—Concepts and Perspectives*; VHC: Weinheim, 1995.
(18) Pauwels, T., F.; Lippens, W.; Smet, P., W.; Herman, G., G.; Goeminne, A., M. *Polyhedron* **1999**, 1029.
(19) Chin, J.; Lee, S. S.; Lee, K., J.; Park, S.; Kim, D., H. *Nature* **1999**, *401*, 254.
(20) Martell, A. E.; Motekaitis, R. J. *J. Am. Chem. Soc.* **1988**, *110*, 8059.
(21) Humphry, T.; Forconi, M.; Williams, N. H.; Hengge, A. C. *J. Am. Chem. Soc.* **2002**, *124*, 14860.
(22) Schubert, U. B.; Heller, M. *Chem. Eur. J.* **2001**, *7*, 5252.
(23) Norsten, T. B.; Frankamp, B. L.; Rotello, V. M. *Nano Lett.* **2002**, *2*, 1345.
(24) Prevot-Halter, I.; Smith, T. J.; Weiss, J. *Tetrahedron Lett.* **1996**, 1201.
(25) Prokopuk, N.; Weinert, C. S.; Siska, D. P.; Stern, C. L.; Shriver, D. F. *Angew. Chem., Int. Ed.* **2000**, *39*, 3312.

10.1021/ic034823b CCC: $25.00
Published on Web 11/14/2003

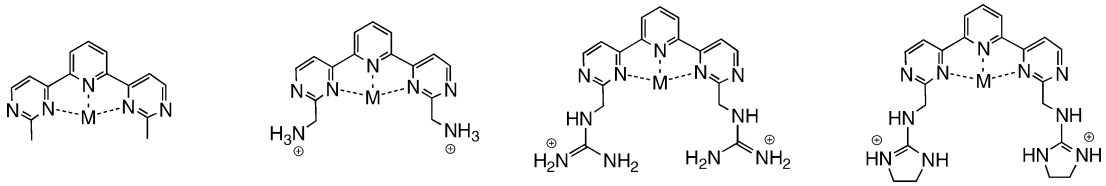

1-M **2-M** **3-M** **4-M**

Figure 1. Metal complexes examined in this study.

Scheme 1. The Complexation of a Metal Ion with a Functionalized 2,6-Di(pyrimidin-4-yl)pyridine Ligand[a]

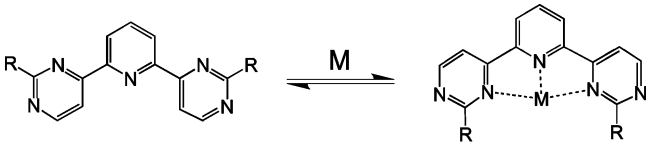

M = Zn(II), Cu(II)

[a] The variable R groups are retained in the proximity of the metal center in the complex. The ligand adopts a folded or "horseshoe" conformation relative to the extended conformation of the free ligand

complex-based catalysts.[3,27] In addition, functionalized inorganic complexes have been used in enzyme active site mimicking,[2,3,21,27] as cooperativity between functional groups and metal ions is thought to be fundamental to the activity of many wild-type enzymes.[28,29]

Derivatives of the 2,6-di(pyrimidin-4-yl)pyridine ligand can be prepared with functionality at the 2 positions of the terminal pyrimidine rings.[30] Coordination to a metal center requires a folded or "horseshoe" ligand conformation relative to the more extended conformation that has been observed for 2,6-di(pyrimidin-4-yl)pyridine by X-ray crystallograpy[30] (see Scheme 1). Metal complexation retains the functionality at the 2 position of the pyrimidine rings in the proximity of the metal center, thus furnishing a cleft in which the metal center and auxiliary groups reside. Such an arrangement would be expected to exploit interactions and cooperativity between the metal center and the auxiliaries. Furthermore, the function of metal coordination as a conformational lock offers the possibility of controlling higher order structure within macromolecular systems in a novel way. In previous studies, we have utilized the 2,6-di(pyrimidin-4-yl)pyridine scaffold to generate a cleft containing Zn(II) and guanidinium auxiliaries for use both in the promotion of RNA hydrolysis[27] and as part of an amino acid sensing ensemble.[31] Herein, the effects of ammonium, guanidinium, and 2-amino-4,5-dihydro-imidazolinium auxiliaries on the stabilities of the Zn(II) and Cu(II) complexes of the 2,6-di(pyrimidin-4-yl)-pyridine derivatives are examined (Figure 1).

Experimental Section

General information. All reagents were obtained from Aldrich and Acros and used without further purification. Dichloromethane and triethylamine were distilled over CaH_2 and used immediately. Ion exchange chromatography was performed with Amberlite IRA-400 (Cl) ion-exchange resin. Compounds **5**,[30] **6**,[32] **8**,[33] and **10**[34] were prepared as previously reported in the literature. A Varian Unity Plus 300 MHz spectrometer was used to obtain ^{1}H and ^{13}C NMR spectra, which are referenced to the solvent. A Finnigan VG analytical ZAB2-E spectrometer was used to obtain high-resolution mass spectra. UV/vis spectra were recorded on a Beckman DU-640 spectrophotometer. All pH measurements were made using an Orion 720A pH meter. A Harvard syringe pump was employed for the potentiometric pH titrations.

Metal Binding Studies. All binding studies were carried out in 0.01 M HEPES buffer at pH 6.8. The metal chloride titrant solutions were prepared by addition of a concentrated metal chloride stock solution into a portion of the analyte solution, ensuring the change in concentration of buffer and host over the course of the titration to be negligible. Experimental data was fit to theoretical curves generated using eq 1,[35] assuming the equilibrium presented in eq 2 to determine formation constants of 1:1 complexes. The concentration of free metal ion [M] is related to known variables and parameters by the quadratic equation given (eq 3).

$$\Delta A = (\Delta\epsilon K_f[M][L]_t)/(1 + K_f[M]) \quad (1)$$

$$[M] + [L] \overset{[K_f]}{\rightleftharpoons} [ML] \quad (2)$$

$$K_f = [ML]/([M][L])$$

$$[M] = -b + (b^2 - \{4K_f\,[M]_t\}^{1/2})/2K_f \quad (3)$$

where $\Delta\epsilon$ = difference in extinction coefficient of complex and ligand, K_f = formation constant of complex, [M] = concentration of free metal, $[M]_t$ = total concentration of metal added to the solution, [L] = concentration of free ligand, $[L]_t$ = total concentration of ligand added to the solution, [ML] = concentration of complex, and $b = 1 - K_f[M]_t + K_f[L]_t$. Ligand concentrations were adjusted according to quantitative ^{1}H NMR measurements using HPLC-grade acetonitrile as an internal standard. A typical titration involved the addition of 2.5 μL aliquots of a solution that was 4.8 mM in metal chloride, 100 μM in ligand, and 10 mM buffer to 1.2 mL of a solution that was 100 μM in ligand and 10 mM buffer. In the phosphate studies, phosphate was introduced to the buffer

(26) Mann, S.; Huttner, G.; Zsolnai, L.; Heinze, K. *Angew. Chem., Int. Ed. Engl.* **1996**, *35*, 2808.
(27) Aït-Haddou, H.; Sumaoka, J.; Wiskur, S.; Folmer-Andersen, F.; Anslyn, E. V. *Angew. Chem., Int. Ed.* **2002**, *41*, 4041.
(28) Kramer, R. *Eur. Coord. Chem. Rev.* **1999**, *182*,1635.
(29) Wilcox, D. *Chem. Rev.* **1996**, *96*, 2435.
(30) Bejan, E.; Aït-Haddou, H.; Duran, J.; Balvoine, G. *Synthesis* **1996**, 1012.
(31) Aït-Haddou, H.; Wiskur, S.; Lynch, V. M.; Anslyn, E. V. *J. Am. Chem. Soc.* **2001**, *123*, 11296.
(32) Lange, U., Schäfer, B., Baucke, D., Buschmann, E., Mack, H. *Tetrahedron. Lett.* **1999**, *40*, 7067.
(33) Bergeron, R., McManis, J. *J. Org. Chem.* **1987**, *52*, 1700.
(34) Mundula, S.; Wilson, L.; Klopfenstein, S.; Seibel, W.; Nikolaides, N. *Tetrahedron Lett.* **2000**, *41*, 6568.
(35) Connor, K. A. *Binding Constants, The Measurement of Molecular Complex Stability*; Wiley-Interscience: New York, 1987; pp 147−149.

solution with dibasic sodium phosphate prior to adjustment of pH and was present in both the analyte and titrant solutions in roughly the same concentration. In all cases, binding isotherms were fit to the theoretical curves by manual variation of parameters.

Potentiometric Titrations. Solutions were made up to be 5.0 mL total volume and were 4.0 mM in ligand or complex and 50 mM in KNO_3. Solutions were adjusted to pH = 2.0 by the addition of 0.1 M nitric acid. Each data point was obtained by the automated addition of 20 μL of a 0.0985 M volumetric standard NaOH to the stirred solution over a period of 20 s followed by a 30 s waiting period during which time the pH meter was allowed to equilibrate.

Synthesis. (4-{6-[2-(*tert*-Butoxycarbonylamino-methyl)pyrimidin-4-yl]pyridin-2-yl}pyrimidin-2-ylmethyl)carbamic Acid *tert*-Butyl Ester (7). Absolute ethanol (100 mL) was heated to 80 °C, followed by the addition of **5** (2.00 g, 7.31 mmol) and **6** (6.10 g, 29.2 mmol). Sodium metal (1.01 g, 43.5 mmol) was dissolved in absolute ethanol (50 mL), and the sodium ethoxide solution was then slowly added to the reaction mixture with a syringe. The reaction mixture was stirred at 80 °C for 16 h and then allowed to cool to room temperature. The purple solution was concentrated to a solid residue, which was dissolved in CH_2Cl_2 (100 mL) and washed with water (3 × 50 mL) and brine (1 × 50 mL). The organic layer was then dried over sodium sulfate and concentrated to give a dark red residue, which was subjected to alumina chromatography (eluent = ethyl acetate) to yield a white solid (1.67 g, 49% yield). Mp: 216−217 °C. ^{1}H NMR ($CDCl_3$): δ 8.86 (d, J = 5.2 Hz, 2H), 8.65 (d, J = 7.8 Hz, 2H), 8.35 (d, J = 5.2 Hz, 2H), 8.06 (t, J = 7.9 Hz, 1H), 5.70 (b, 2H), 4.72 (d, J = 5.0 Hz, 4H), 1.51 (s, 18H). ^{13}C NMR ($CDCl_3$): δ 166.3, 162.3, 158.1, 156.1, 153.3, 138.3, 123.4, 115.3, 79.5, 46.4, 28.4. HRMS (CI, *m*/*z*): calcd for $C_{25}H_{31}N_7O_4$ 494.252, found 494.251.

***C*-{4-[6-(2-Aminomethyl-pyrimidin-4-yl)pyridin-2-yl]pyrimidin-2-yl}methylamine Dihydrochloride (2).** To a solution of 9:1 by volume CH_2Cl_2:TFA(trifluoroacetic acid) (10 mL) was added **7** (1.00 g, 2.13 mmol). The reaction mixture was stirred vigorously for 24 h at 25 °C, and the solvent was removed under reduced pressure to give a yellow oil. Excess TFA was azeotroped using toluene under reduced pressure, yielding a pale yellow solid. The product was precipitated in chilled ethanol, filtered, washed with diethyl ether, and dried under high vacuum. Ion exchange chromatography yielded a white solid (0.74 g, 94% yield). Mp: 228−229 °C. ^{1}H NMR (CD_3OD): δ 8.86 (d, J = 5.2 Hz, 2H), 8.64 (d, J = 7.9 Hz, 2H), 8.34 (d, J = 5.2 Hz, 2H), 8.04 (t, J = 7.9 Hz, 1H), 4.20 (s, 4H). ^{13}C NMR (CD_3OD): δ 163.3, 162.5, 159.7, 153.1, 140.1, 125.1, 117.5, 44.1. HRMS (CI, *m*/*z*): calcd for $C_{15}H_{15}N_7$ 294.147, found 294.148.

***N*-{4-[6-(2-*tert*-Butoxycarbonyl-guanidinomethyl-pyrimidin-4-yl)pyridin-2-yl]pyrimidin-2-ylmethyl}-*tert*-butoxycarbonyl-guanidine (9).** To a 9:1 by volume solution of CH_2Cl_2: DMF (10 mL) was added triethylamine (0.4 mL, 2.82 mmol) followed by **2** (0.41 g, 1.13 mmol) and **8** (0.821 g, 2.82 mmol). The heterogeneous reaction mixture was stirred at 25 °C for 24 h. The reaction was then diluted with CH_2Cl_2 (50 mL) and washed with water (3 × 25 mL) and brine (2 × 25 mL). The organic layer was dried over sodium sulfate and concentrated to a pale yellow solid. The product was precipitated in chilled methanol, filtered, washed with diethyl ether, and dried under high vacuum to yield a white solid (0.39 g, 42% yield). Mp: 240−241 °C. ^{1}H NMR ($CDCl_3$): δ 11.58 (b, 2H) 9.92, (b, 2H), 8.92 (d, J = 5.2 Hz, 2H), 8.88 (d, J = 7.9 Hz, 2H) 8.44 (d, J = 5.2 Hz, 2H), 8.02 (t, J = 7.9 Hz, 1H), 4.99 (d, J = 4.0 Hz, 4H), 1.57 (s, 16H) 1.53 (s, 16H). ^{13}C NMR ($CDCl_3$): δ 164.90, 163.59, 162.15, 158.70, 155.70, 153.23, 138.35, 123.93, 115.25, 80.01, 79.41, 46.70, 28.26, 28.09. HRMS (CI, *m*/*z*): calcd for $C_{37}H_{51}N_{11}O_8$ 778.328, found 778.323.

***N*-{4-[6-(2-Guanidinomethyl-pyrimidin-4-yl)pyridin-2-yl]pyrimidin-2-ylmethyl}guanidine Dihydrochloride (3).** To a 2:1 by volume solution of CH_2Cl_2:TFA (10 mL) was added **9** (0.36 g, 0.47 mmol). The reaction mixture was stirred at 25 °C for 8 h, after which a dark red oil was observed. The reaction mixture was concentrated to an off-white solid, and excess TFA was azeotroped using toluene. The product was precipitated in chilled ethanol, filtered, washed with diethyl ether, and dried under high vacuum. Ion exchange chromatography gave a white solid (0.27 g, 93% yield). Mp: 232−233 °C. ^{1}H NMR (CD_3OD): δ 8.82 (d, J = 5.3 Hz, 2H), 8.46 (d, J = 7.8 Hz, 2H), 8.33 (d, J = 5.3 Hz, 2H), 8.06 (t, J = 7.9 Hz, 1H), 4.43 (s, 4H). ^{13}C NMR (CD_3OD): δ 166.07, 164.17, 162.87, 160.15, 154.71, 140.17, 125.10, 117.15, 47.73. HRMS (CI, *m*/*z*): calcd for $C_{31}H_{39}N_{11}O_4$ 378.191, found 378.190.

***N*-{4-[6-(2-*tert*-Butoxycarbonyl-imidazolinomethyl-pyrimidin-4-yl)pyridin-2-yl]pyrimidin-2-ylmethyl}-*tert*-butoxycarbonyl-imidazoline (11).** To a 9:1 ethanol:acetic acid solution were added **2 (**1.04 g, 2.85 mmol) and **10** (1.55 g, 7.11 mmol). The reaction mixture was heated to 50 °C for 24 h. Triethylamine (3 mL, 21.52 mmol) was added, and the reaction mixture was concentrated to a pale yellow solid, which was dissolved in 100 mL of CH_2Cl_2. This solution was washed with 1 M $NaOH_{(aq)}$ (2 × 50 mL) water (50 mL) and brine (50 mL), dried over sodium sulfate, and concentrated to a white solid. The product was precipitated in methanol, filtered, washed with diethyl ether, and dried under high vacuum to yield a white solid (0.76 g, 42% yield). ^{1}H NMR ($CDCl_3$): δ 8.89 (d, J = 5.1 Hz, 2H), 8.81 (d, J = 7.5 Hz, 2H), 8.38 (d, J = 5.4 Hz, 2H), 8.29 (b, 2H), 8.06 (t, J = 7.8 Hz, 1H), 4.82 (d, J = 4.4 Hz, 4H). ^{13}C NMR ($CDCl_3$): δ166.34, 162.51, 158.81, 154.05, 153.65, 153.13, 138.64, 124.10, 115.405, 82.24, 49.30, 48.46, 47.15, 28.58. HRMS (CI, *m*/*z*): calcd for $C_{31}H_{39}N_{11}O_4$ 630.326, found 630.326.

***N*-{4-[6-(2-Imidazolinomethyl-pyrimidin-4-yl)pyridin-2-yl]pyrimidin-2-ylmethyl}imidazoline Dihydrochloride (4).** To a 2:1 by volume solution of freshly distilled CH_2Cl_2:TFA (10 mL) was added **11** (0.36 g, 0.58 mmol). Vigorous stirring of the solution for 8 h at 25 °C resulted in the formation of a dark red oil. The reaction mixture was concentrated under reduced pressure to give a red oil. TFA was azeotroped using toluene until a dark red solid precipitated. Ion exchange chromatography gave a pale yellow solid (0.26 g, 89% yield). Crystals suitable for X-ray crystallography were obtained by slow diffusion of ethanol into a concentrated methanol solution. Mp: 236−237 °C. ^{1}H NMR (CD_3OD): δ 8.89 (d, J = 5.1 Hz, 2H), 8.71 (d, J = 8.1 Hz, 2H), 8.56 (d, J = 5.1 Hz, 2H), 8.17 (t, J = 8.1 Hz 1H), 4.72 (s, 4H), 3.80 (t, J = 1.5 Hz, 8H). ^{13}C NMR (CD_3OD): δ 166.18, 164.25, 162.27, 160.25, 154.82, 140.23, 124.81, 117.24, 44.30. HRMS (CI): calcd for $C_{21}H_{25}N_{11}Cl_2$ 501.167, found 501.165.

[1-Zn(Cl)$_2$]. To refluxing anhydrous methanol (3 mL) was added **1** (0.100 g, 0.38 mmol), and the reaction mixture was stirred until homogeneous. A 1 M aqueous solution of $ZnCl_2$ (380 μL, 1 equiv) was injected, and the solution was allowed to cool to room temperature, effecting the precipitation of a pale yellow solid. The solid was filtered, washed with cold methanol, and recrystallized from methylene chloride to give white crystals suitable for X-ray crystallography (0.093 g, 61% yield). ^{1}H NMR ($CDCl_3$): δ 9.07 (d, J = 5.1 Hz, 2H), 8.47 (s, 3H), 7.96 (d, J = 5.1 Hz, 2H), 3.41 (s, 6H), ^{13}C NMR (CD_3OD): δ 170.76, 160.88, 154.17, 149.53, 143.40, 125.07, 114.54, 26.19.

[3-Zn(Cl$_2$)]ZnCl$_4$. To deionized water (25 mL) was added **3** (0.46 g, 1.01 mmol) and $ZnCl_2$ (0.515 g, 3.75 equiv). The pale yellow solution was heated to 80 °C for 24 h. The solution was

Scheme 2[a]

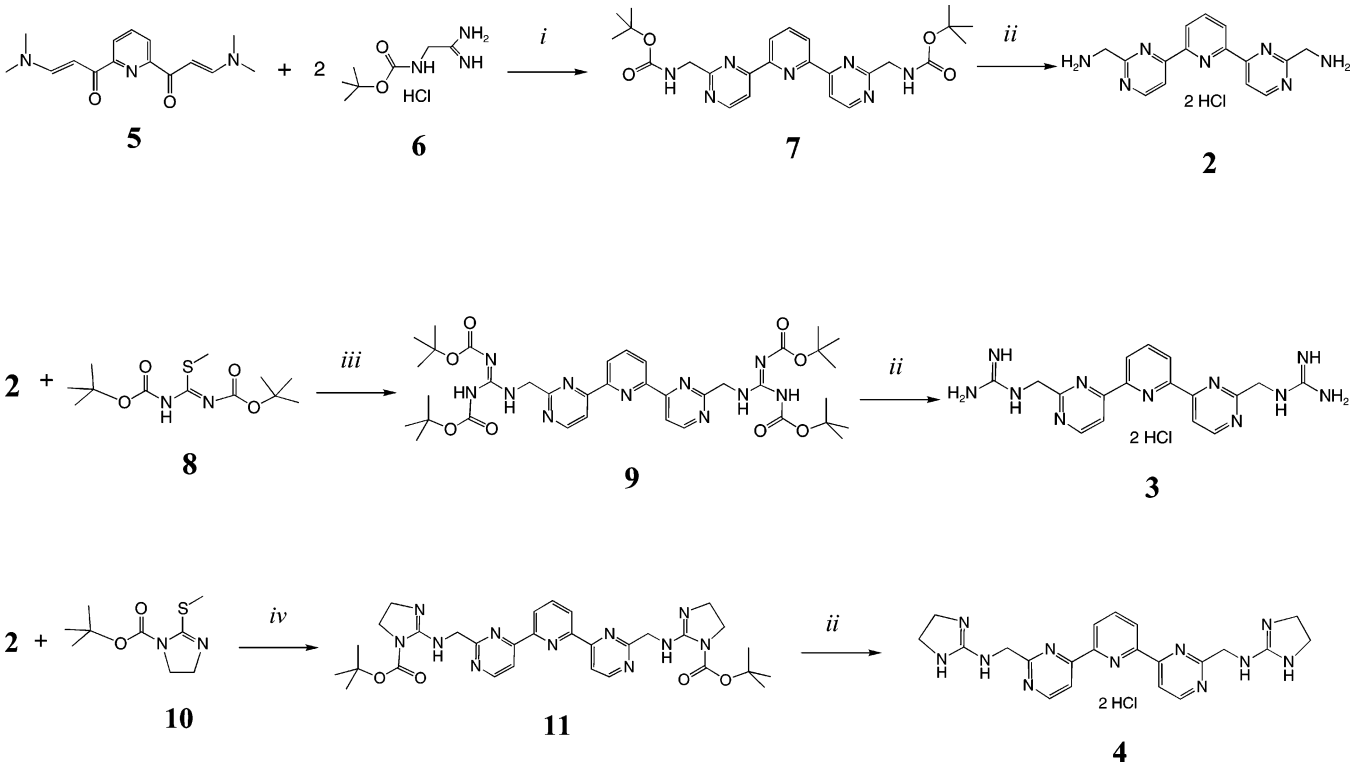

[a] Reagents and conditions: (i) EtOH/NaOEt, 80 °C; (ii) TFA, CH_2Cl_2; (iii) CH_2Cl_2, DMF, Et_3N; (iv) EtOH, AcOH, 50 °C.

then filtered and lyophilized. The resulting solid was crystallized from methanol:water (99:1) by slow evaporation to yield pale yellow crystals suitable for X-ray crystallography (0.61 g, 80% yield). ^{1}H NMR (CD_3OD): δ 9.40 (d, J = 5.4 Hz, 2H), 9.06 (d, J = 8.2 Hz, 2H), 8.82 (t, J = 8.2 Hz, 1H), 8.75 (d, J = 5.4 Hz, 2H), 5.01 (d, 4H). ^{13}C NMR (CD_3OD): 166.37, 163.09, 159.28 157.43, 148.44, 145.22, 127.96, 118.56, 48.14.

[4-Zn(Cl$_2$)]ZnCl$_4$. To deionized water (15 mL) was added **4** (0.35 g, 0.69 mmol) and $ZnCl_2$ (0.31 g, 2.29 mmol). The pale yellow solution was filtered and lyophilized. The resulting pale yellow solid was dissolved in the minimum amount of methanol with heat and sonication, hot filtered, and allowed to cool to room temperature to yield large, pale yellow crystals suitable for X-ray crystallography (0.39 g, 77% yield). ^{1}H NMR (CD_3OD): δ 9.12 (d, J = 5.5 Hz, 2H), 8.81 (d, J = 7.5 Hz, 2H), 8.58 (t, J = 7.5 Hz, 1H), 8.44 (d, J = 5.5 Hz, 2H), 5.09 (s, 4H), 3.68 (s, 8H). ^{13}C NMR (CD_3OD): 165.28, 163.01, 156.11, 147.96, 144.88, 127.24, 117.68, 47.32, 43.12.

Crystal Structure Determination. The data were collected on a Nonius Kappa CCD diffractometer using a graphite monochromator with Mo Kα radiation (λ = 0.71073 Å). The data were collected at 153 K using an Oxford Cryostream low-temperature device.. Data reduction were performed using DENZO-SMN. The structure was solved by direct methods using SIR92 and refined by full-matrix least-squares on F^2 with anisotropic displacement parameters for the non-H atoms using SHELXL-97. The hydrogen atoms were calculated in ideal positions with isotropic displacement parameters set to 1.2U_{eq} of the attached atom (1.5U_{eq} for methyl hydrogen atoms). Selected bond lengths may be found in Table 1. Additional information may be found in the Supporting Information.

Results and Discussion

Synthesis. Ligands **2**−**4** were synthesized by the route shown in Scheme 2. The bis-enaminone **5** was condensed with *tert*-butyl carbamate (Boc) protected amino amidine **6** to give the Boc-protected amino functionalized ligand **7**. The protective groups were removed with trifluoroacetic acid (TFA) to give **2**. The auxiliary amines of **2** were converted to guanidinium groups by reaction with Boc-protected pseudomethoxythiourea **8** in 9:1 methylene chloride:*N*,*N*-dimethylformamide solution in the presence of triethylamine.

Table 1. Selected Bond Lengths (Å) for Zn(II) Complexes of Various Ligands Determined by X-ray Crystallography

ligand	Zn−N(8)	Zn−N(1)	Zn−N(14)	Zn−Cl(1)	Zn−Cl(2)
1	2.082	2.262	2.234	2.244	2.233
3	2.077	2.265	2.211	2.273	2.252
4	2.065	2.253	2.225	2.241	2.281
tpy	2.106	2.185	2.185	2.282	2.282

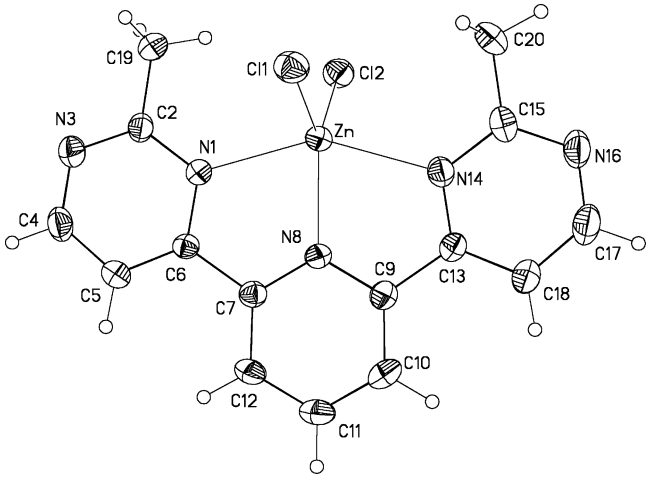

Figure 2. View of [**1**-**Zn**(Cl$_2$)] showing the atom-labeling scheme. Displacement ellipsoids are scaled to the 50% probability level.

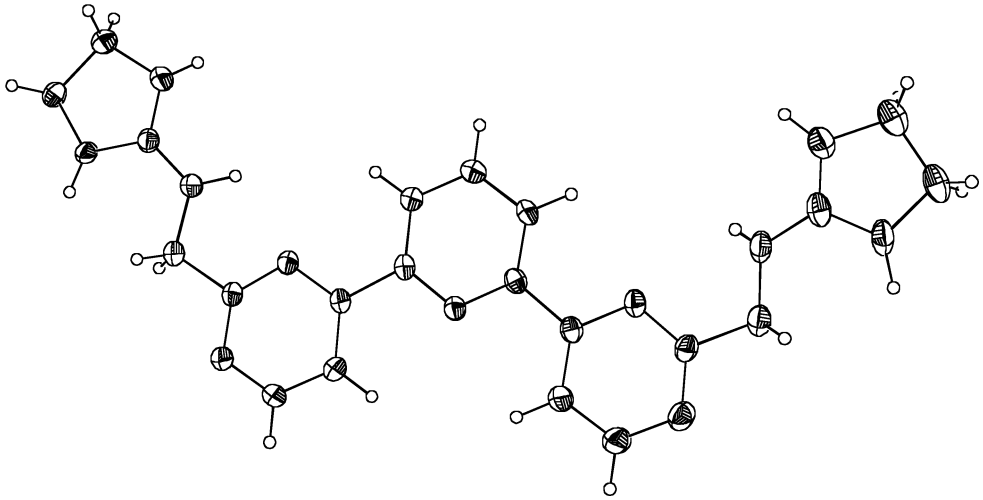

Figure 3. View of the cationic portion of **4**. Displacement parameters have been scaled to the 50% probability level.

The protective groups were removed, yielding **3**. Ligand **4** was obtained from **2** by reaction with Boc-protected imidazoline pseudomethoxythiourea **10** according to literature procedure[34] followed by removal of the protective groups. The dimethyl ligand **3** was prepared as previously reported.[30] Recrystallization of ligands **1**, **3**, and **4** from methanol in the presence of excess $ZnCl_2$ provided [**1-Zn**(Cl_2)], [**3-Zn**(Cl_2)]-$ZnCl_4$, and [**4-Zn**(Cl_2)]$ZnCl_4$.

X-ray Crystal Structures. The X-ray crystal structure of [**1-Zn**(Cl_2)] is shown in Figure 2. The Zn(II) complex exhibits distorted trigonal bypyramidal geometry about the Zn(II) center. The Zn−N(8) bond length is 2.082 Å, which is significantly shorter than the Zn−N(1) and Zn−N(14) bonds (2.262 and 2.234 Å, respectively). A shorter Zn−N bond to the central pyridine nitrogen than to the nitrogens of the terminal rings has been observed for the Zn(II) complex of 2,2′,6′,2″-terpyridine (**tpy-Zn**),[36] although in the case of [**1-Zn**(Cl_2)] the effect is more dramatic. This may be due to inductive electron withdrawal by N(3) and N(16), decreasing the Lewis basicity of the terminal pyrimidine rings. Steric repulsion between the methyl groups could also contribute to this effect. The bond lengths to the Zn(II) center observed in all complexes determined as well as **tpy-Zn** are shown in Table 1. The integrity of the Zn(II) coordination geometry is not compromised by the presence of the cationic auxiliary groups.

The crystal structures of **4** and **4-Zn** are shown in Figures 3 and 4, respectively. The free ligand in Figure 3 adopts an extended conformation in the solid state in which the distance between the two cationic 2-amino-4,5-dihydro-imidazolinium groups is maximized and endocyclic nitrogen lone pair interactions are minimized. A similar solid-state conformation has been observed for the parent 2,6-di(pyrimidin-4-yl)-pyridine core (R = H in Scheme 1).[30] The structure of **4-Zn** in Figure 4 shows the complex to have coordination geometry similar to that of **1-Zn**. The ligand is oriented with the auxiliaries pointed away from each other, presumably to minimize electrostatic repulsions present in the complex. This creates a well-defined twist in the core, with a C(5), C(6), C(7), C(12) dihedral angle of 5.14° and a C(10), C(9), C(13), C(18) dihedral angle of 4.57°. The observed conformation provides a somewhat C_2-symmetric appearance in the complex.

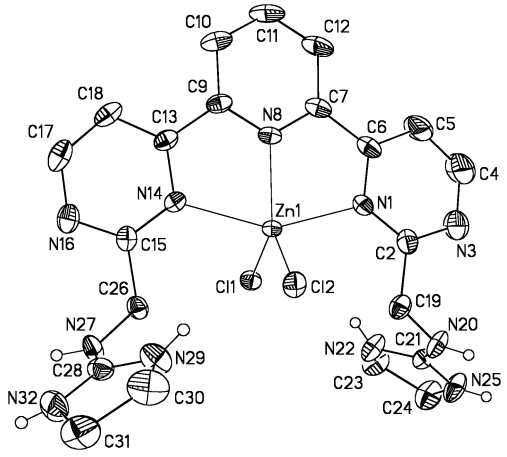

Figure 4. View of [**4-Zn**(Cl_2)]$^{2+}$ showing the atom-labeling scheme. Displacement ellipsoids are scaled to the 50% probability level. Most hydrogen atoms have been removed for clarity.

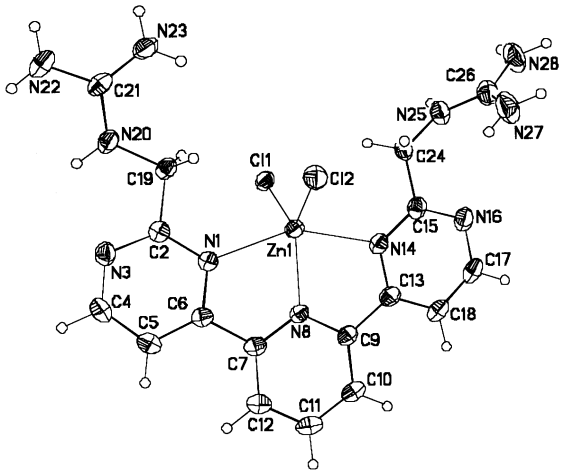

Figure 5. View of [**3-Zn**(Cl_2)]$^{2+}$ showing the atom-labeling scheme. Displacement ellipsoids are scaled to the 50% probability level.

(36) Vlasser, M.; Rojo, T.; Beltran-Porter, D. *Acta Crystallogr.* **1983**, *C39*, 560.

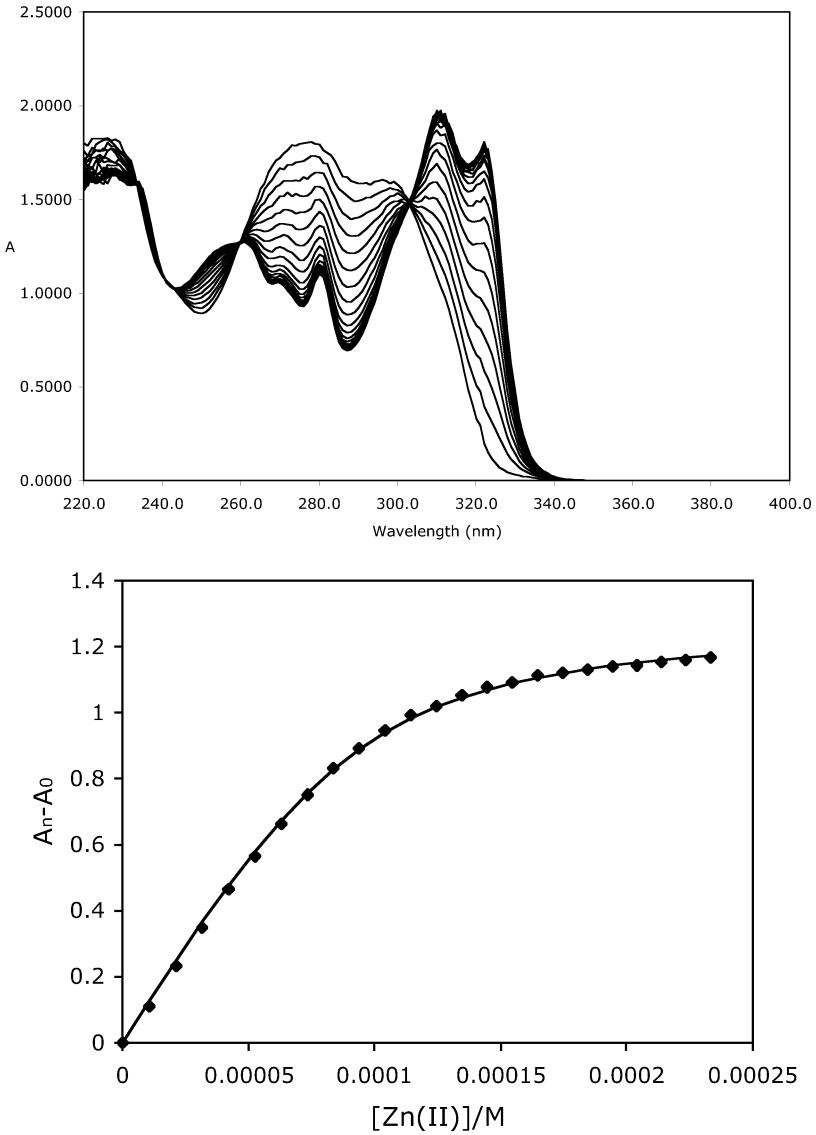

Figure 6. Representative UV/vis data (a) and binding isotherm for changes in absorbance at 325 nm (b). Experiments were carried out in 0.01 M HEPES at pH = 6.8 with 100 μM ligand. Metal chloride salts were added in increments of 0.1 equiv. For the binding isotherm, the dots are the experimental data and the line is the theoretical curve calculated from eq 1.

The X-ray crystal structure of **3-Zn** is shown in Figure 5. The Zn−N bond lengths and coordination geometry about the Zn(II) center are similar to those of **1-Zn** and **4-Zn**. The guanidinium auxiliary groups would be expected to have greater hydrogen-bonding ability than to the more hindered 2-amino-4,5-dihydro-imidazolinium groups of **4-Zn** as is exhibited by the incorporation of multiple solvent molecules that are hydrogen bonded to the guanidinium auxiliaries. This establishes a less-ordered orientation of the guanidinium auxiliaries with respect to the 2,6-di(pyrimidin-4-yl)pyridine core than is observed for **4-Zn**. In the **3-Zn** structure, the position of the auxiliaries is dictated primarily by intermolecular hydrogen bonding as opposed to intramolecular electrostatic repulsions as in **4-Zn**, and, as a result, **3-Zn** adopts a less symmetric solid-state geometry than **4-Zn**.

Metal Binding Studies. The nature of the variable groups appended to the 2,6-di(pyrimidin-4-yl)pyridine core could be expected to have pronounced effects on the stability of the transition metal complexes formed.[37] Steric and electrostatic interactions between the auxiliary groups will be augmented upon metal binding due to their close proximity in the chelated conformation relative to the extended conformation of the unbound ligand. Additionally, electrostatic interactions between charged auxiliary groups and the metal center may also be of importance in determining complex stability. The aforementioned interactions are thought to be responsible for the orientation of **4-Zn** exhibited in Figures 4.

The UV/vis spectrum of **1** in buffered aqueous solution at pH = 6.8 exhibits a broad maximum at 275 nm with a shoulder at 291 nm. The presence of auxiliary functional groups of **2**−**4** has only a subtle effect on the spectra, causing a slight sharpening of the peaks and a slight hypsochromic shift in the shoulder to 295 nm in all cases. The absorbance spectra of all ligands are greatly modulated by the addition of Cu(II) or Zn(II), leading to the appearance of two sharper

(37) Crans, D. C.; Boukhobza, I. *J. Am. Chem. Soc.* **1998**, *120*, 8069.

Scheme 3. Coordination of the Auxiliary Amines of **2** to the Zn(II) Center Provides an Explanation for the Large Complex Stability of **2-Zn**

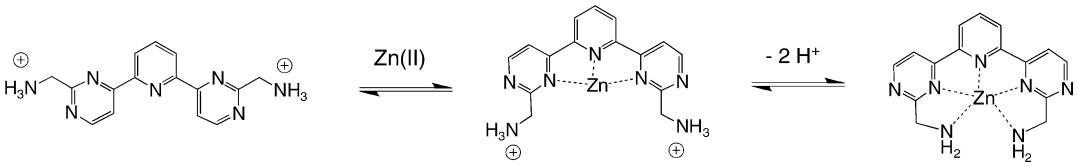

Table 2. Formation Constants of Various Ligand Metal Complexes in Aqueous Solution at pH = 6.8 as Determined by UV/Vis Spectrophotometric Titration

ligand	metal	stoichiometry	K (M^{-1})
1	Cu(II)	1:1	1×10^6
1	Zn(II)	1:1	8.4×10^3
2	Cu(II)	not 1:1	nd[a]
2	Zn(II)	1:1	4.5×10^5
3	Cu(II)	1:1	7.8×10^4
3	Zn(II)	1:1	<100
4	Cu(II)	1:1	4.1×10^4
4	Zn(II)	1:1	<100
tpy	Cu(II)	1:1	1.6×10^{13}
tpy	Zn(II)	1:1	1×10^6

[a] Not determined.

maxima that are red-shifted with respect to the free ligand absorbances (320 and 331 nm for Cu(II) complexes and 313 and 327 nm for Zn(II) complexes). Clear isosbestic points are observed over the course of this process (307 and 265 nm for Cu(II) complexes and 303 nm for Zn(II) complexes). Formation constants were determined assuming 1:1 binding by curve-fitting analysis (see Experimental Section). A representative UV/vis titration and binding isotherm are presented in Figure 6.

The determined formation constants for the Zn(II) and Cu(II) complexes of the ligands studied are presented in Table 2. Previously determined values obtained from the literature[38] for tpy are included to provide an estimation of the effects of the noncoordinating, endocyclic nitrogens and the exocyclic substituents.

It is apparent that the auxiliary nitrogen-containing functional groups dramatically affect the stability of the complexes. The low stability of the Cu(II) and Zn(II) complexes of **3** and **4** relative to those of **1** can be explained in terms of electrostatic repulsions between the charged guanidinium and 2-amino-4,5-dihydro-imidazolinium groups and the metal center, as suggested by the X-ray structure of **4-Zn**. It is also likely that inductive electron withdrawal by the positively charged auxiliaries decreases electron density in the ligand core, reducing its ability to act as a Lewis base.

Interestingly, the formation constant for complex **2-Zn** is significantly larger than for **1-Zn**. The large formation constant of **2-Zn** implies that the auxiliary amines of **2** could be taking part in the coordination chemistry by coordinating to the bound Zn(II) ion as shown in Scheme 3. Such behavior is not likely with the metal complexes of **3** and **4** due to the much weaker acidity of guanidinium[39] and 2-amino-4,5-dihydro-imidazolinium (which is essentially a substituted guanidinium) groups. The formation constant for complex **2-Cu** could not be determined because a second spectral change emerged immediately after the addition of more than 1 equiv of copper to the ligand. This interfered with the saturation portion of the binding isotherm, making the curve-fitting process impossible. Such behavior suggests the formation of higher order aggregates in which multiple Cu(II) ions are bound to each ligand.

Potentiometric Studies. The postulated coordination of the auxiliary amines of **2** to the Zn(II) center in **2-Zn** would be expected to appreciably increase the acidity of the corresponding ammoniums.[40,41] In fact, such an effect is observed. Overlaid potentiometric titrations of **2** and **2-Zn** are shown in Figure 7. The titration curve for the free ligand **2** shows a buffering region of 2 equiv corresponding to an acidic group with a pK_a just below 9.0, which is assigned to the auxiliary amines. The presence of 1 equiv of $ZnCl_2$ causes this buffering region to fall to about 5.5, corresponding to a depression of roughly 3.5 pK_a units upon Zn(II) complexation. The stability constant determinations were carried out at pH = 6.8, at which the auxiliary amines would be deprotonated and presumably coordinated to the Zn(II) center.

Phosphate Effects. The cationic nitrogen-containing auxiliaries of **2**−**4** are hydrogen bond donors and potential sites for charge-pairing recognition. Intermolecular interactions of these types with an anionic, hydrogen bond acceptor should increase metal complex stability in cases where electrostatic repulsions between multiple cationic groups are responsible for low stability, as is thought to be the case with **3-Zn** and **4-Zn**.

It was observed that the presence of exogenous phosphate causes a large increase in the stability of the **3-Zn**, but not in the stability of **1-Zn** (**2-Zn** and **4-Zn** were not examined). Formation constants for **1-Zn** and **3-Zn** were determined in the presence of 1 equiv of Na_2HPO_4 by the UV/vis method previously described. The formation constant for **3-Zn** increased from >100 M^{-1} in the absence of phosphate to 4300 M^{-1}, at least an increase of over 40-fold, while the formation constant of **1-Zn** increased from 8300 to 8900 M^{-1}, which is less than a factor of 1.1. The stabilizing effect of the presence of the phosphate anion can be attributed to charge pairing and hydrogen bonding of phosphate with guanidinium functionalities of **3** as shown in Figure 8. Interactions between guanidinium groups and phosphate groups have previously been demonstrated in molecular recognition applications in aqueous solution.[42] The associa-

(38) Martell, A. E.; Smith, R. M. *Critical Stability Constants Volume 5: First Supplement*; Plenum Press: New York, 1982; p 253.
(39) Gund, P. *J. Chem. Educ.* **1972**, *49*, 100.
(40) Reichenbach-Klinke, R.; Zabel, M.; König. *J. Chem. Soc., Dalton Trans.* **2003**, *1*, 141.
(41) Rothermel, G. L.; Miao, L.; Hill, A. L.; Jackels, S. C. *Inorg. Chem.* **1992**, *31*, 4859.
(42) Kato, Y.; Conn, M, M,; Rebek, J. *J. Am. Chem. Soc.* **1994**, *116*, 3279.

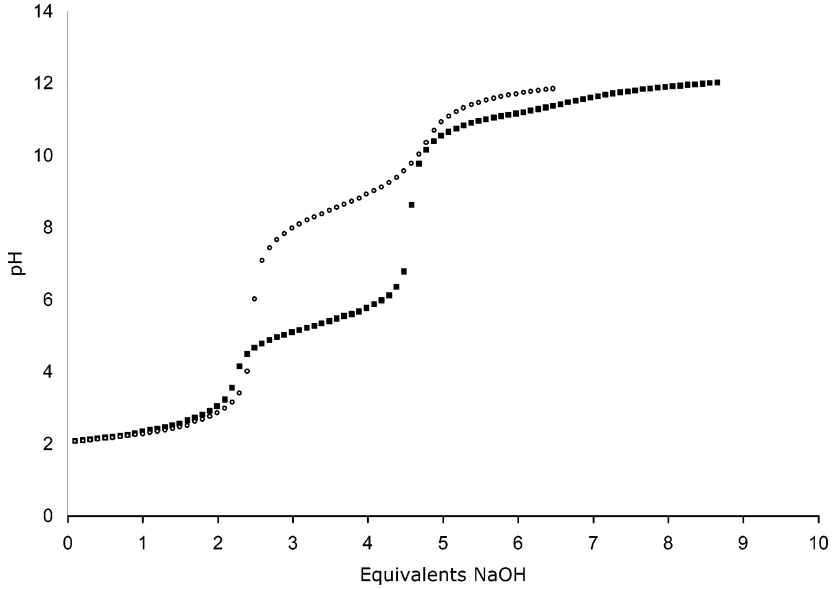

Figure 7. A set of potentiometric pH titrations showing a depression of about 3.5 pK_a units of the auxiliary ammoniums of **2** (○) upon formation of **2-Zn** (■). Each solution contained 20 μmol of analyte and 250 μmol of KNO_3. NaOH was used as the titrant.

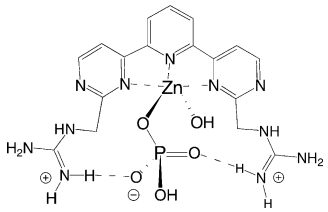

Figure 8. Coordination of the phosphate anion to the Zn(II) center and hydrogen bonding to the auxiliary guanidinium groups provides an explanation for the large increase in the formation constant of **3-Zn** in the presence of phosphate.

tion of phosphate with **3-Zn** would partially offset the four cationic charges that are likely responsible for the low stability of **3-Zn**.

Conclusion

The stability constants of Cu(II) and Zn(II) complexes of ligands **1**− **4** in aqueous solution have been determined. The auxiliary amine groups of **2** are found to largely increase the stability of the Zn(II) complex relative to that of **1**, while auxiliary guanidinium and 2-amino-4,5-dihydro-imidazolinium groups of **3** and **4** have the opposite effect. The presence of the phosphate anion was found to greatly increase the stability of **3-Zn** but to only slightly increase the stability of **1-Zn**. This is likely a consequence of hydrogen-bonding and charge-pairing interactions between the guanidinium groups of **3** and the exogenous phosphate.

Acknowledgment. We gratefully acknowledge support for this work from the National Institutes of Health (GM57306) and the National Science Foundation.

Supporting Information Available: Figures S1−8 showing UV/vis titrations and binding isotherms for formation constant determination of Cu(II) and Zn(II) complexes. Table S1 showing crystallographic information for the determined X-ray crystal structures. CIF files for the determined X-ray crystal structures. This material is available free of charge via the Internet at http://pubs.acs.org.

IC034823B